

## Performance of solar funnel cookers using intermediate temperature test load under low sun elevation

Xabier Apaolaza-Pagoaga<sup>a, \*</sup>, Atul A. Sagade<sup>b, \*</sup>, Celestino Rodrigues Ruivo<sup>c, d, \*</sup>, Antonio Carrillo-Andrés<sup>a, \*</sup>

<sup>a</sup> Energy Research Group, Department of Mechanical, Thermal and Fluids Engineering, University of Malaga, Calle Arquitecto Francisco Peñalosa, 6, 29071 Malaga, Spain

<sup>b</sup> Energy Center, FCFM, University of Chile, Santiago, Chile

<sup>c</sup> Department of Mechanical Engineering, Institute of Engineering, University of Algarve, Campus da Penha, 8005-139 Faro, Portugal

<sup>d</sup> ADAI - LAETA, Rua Pedro Hispano n° 12, 3030-289 Coimbra, Portugal

### ARTICLE INFO

#### Keywords:

Solar funnel cookers  
Sustainable development goals  
Intermediate temperature cooking  
Portable solar cookers  
Clean and sustainable cooking

### ABSTRACT

Solar funnel cookers can be designed as attractive and affordable low-cost devices accessible to people in all continents of the world regardless of their walk-in life. The present work is aimed to investigate the applicability of funnel cookers to attain the temperature in excess of the boiling point of water. It widens their acceptability for cooking and opens new opportunities for technological developments in such designs of solar cookers. Two identical designs of funnel cookers, FC1 and FC2, have been tested with appropriately sized identical cooking pots and glass enclosure to serve the purpose. Cooker FC2 is tested with a glass enclosure only, while a glass enclosure is not used in FC1. Glycerine is used as a test load. Cooker Opto-thermal Ratio (COR) as a thermal performance parameter and overall cooking efficiency are used to compare the performance of the two funnel cookers. It is shown that the temperature of the test load in the cooker FC2 can reach 140 to 150 °C. So, this funnel cooker design can be preferred for cooking food at a relatively high temperature over the boiling point of water. The experimental results show that: i) the mean values of the Cooker Opto-thermal Ratio for cookers FC2 and FC1 are estimated to be 0.157 and 0.110, respectively, and ii) the values of the overall cooking efficiency for cookers FC2 and FC1 are estimated to be 11.8% and 10.2%, respectively.

### Nomenclature

$A_p$	Aperture area of the cooker (m <sup>2</sup> )
$C$	Concentration ratio (-)
$COR$	Cooker opto-thermal ratio ((m <sup>2</sup> °C)/W)
$(M_f C_{pf})'_f$	Sum of thermal capacitances of test load (glycerine) and the cooking pot along with lid (J/°C)
$F'$	Heat exchange efficiency factor
$F' \eta_o$	Optical efficiency factor
$F' U_l$	Overall heat loss factor (W/(m <sup>2</sup> °C))
$G_T$	Global solar irradiance (W/m <sup>2</sup> )
$\bar{G}_T$	Average global solar irradiance for the interval of experiment on the given day (W/m <sup>2</sup> )

$\dot{Q}''$	Rate of useful heat gain by the test load per unit cooker aperture area (W/m <sup>2</sup> )
$T_a$	Temperature of ambient air (°C)
$\bar{T}_a$	Average temperature of ambient air for the interval of experiment on the given day (°C)
$T_{f1}$	Initial temperature of test load (Fitted) (°C)
$T_{f2}$	Final temperature of test load (Fitted) (°C)
$T_{fm}$	Mean temperature of the test load (Fitted) (°C)
$T_{fmax}$	Theoretical maximum achievable fluid temperature (°C)
$T_{Gly}$	Temperature of glycerine (°C)
$T_{(Gly)m}$	Mean temperature of glycerine (°C)
$T_{gst}$	Temperature of stagnation attained by glycerine (°C)

\* Corresponding authors at: Department of Mechanical Engineering, Institute of Engineering, University of Algarve, Campus da Penha, 8005-139 Faro, Portugal (C. Rodrigues Ruivo).

E-mail addresses: [apaolaza@uma.es](mailto:apaolaza@uma.es) (X. Apaolaza-Pagoaga), [atulsagade@gmail.com](mailto:atulsagade@gmail.com) (A.A. Sagade), [cruivo@ualg.pt](mailto:cruivo@ualg.pt) (C. Rodrigues Ruivo), [acarrillo@uma.es](mailto:acarrillo@uma.es) (A. Carrillo-Andrés).

<https://doi.org/10.1016/j.solener.2021.08.006>

Received 15 February 2021; Received in revised form 25 July 2021; Accepted 1 August 2021  
0038-092/© 2021

$U_l$  Heat loss factor (W/(m<sup>2</sup>C))

### Greek symbols

$\tau_R$  Reference time (seconds)  
 $\Delta t$  Time interval (seconds) (unless otherwise specified)  
 $\eta_o$  Optical efficiency  
 $\eta$  Overall cooker efficiency

### Abbreviations

FC1 Funnel solar cooker no. 1  
 FC2 Funnel solar cooker no. 2

## 1. Introduction

United Nations sustainable energy goals inducted the solar cookers as one of the important devices to provide clean energy for all (UN, 2021). Solar energy-based cooking is an established field for decades, and diverse designs of solar cookers have been developed. Many of designs are reported in the literature (Mullick et al., 1987; Tiwari and Yadav, 1986; Grupp et al., 1991; Nandwani and Gomez, 1993; El-Sebaei, 1997; Algifri et al., 2001; Jaramillo et al., 2007; Mirdha and Dhariwal, 2008; Kurt et al., 2008; Harmim et al., 2012a,b; Sethi et al., 2014; Coccia et al., 2017; Cuce, 2018; (Singh and Sethi, 2018) Singh and Sethi, 2018; Saxena et al., 2018; and Sagade et al., 2018a) operate at low temperature (i.e., up to 95–100 °C). However, many food processes (frying, baking, roasting, etc.) need intermediate temperatures (120–240 °C). Different studies reported by Balzar et al., 1996; Stumpf et al., 2001; Mehmet Esen, 2004; Hussein et al., 2008; Kim et al., 2013; Singh et al., 2015; Craig and Dobson, 2017; (Edmonds, 2018) Ian Edmonds, 2018; Sagade et al., 2018b; and Mawire et al., 2020 assessed the ability of solar cookers to attain intermediate temperatures by incorporating different modifications and improving designs. Also, recent modified and advanced designs of solar cookers have been reported in the literature by several researchers such as Zamani et al., 2017; Zhao et al., 2018; Abd-Elhady et al., 2019; Hosseinzadeh et al., 2020; Coccia et al., 2020; Cuce et al., 2020; Saxena et al. 2020; Anilkumar et al., 2020 and Thamizharasu et al., 2020 enhance the propagation of solar cooking sector to the common people. Also, most recently, Singh, 2021; Arif et al., 2021 and Tawfik et al., 2021 have reported the performance of novel designs of solar cookers in India and Egypt.

Also, several studies are available in the literature on different designs of solar panel cookers tested at low temperatures using water as a test load. Solar panel cookers in funnel configuration are made of multiple panel reflectors can be classified as a panel-type solar cooker. Out of these designs, solar panel-type cookers are generally suitable for a slow cooking process. They provide different advantages such as i) simple design; ii) ease of construction and use of inexpensive and locally available materials; iii) minimal need of tracking the sun; iv) easy of operation, handling, transport, and shipping and v) low risk of burning the food. Because of these advantages of solar panel type cookers, several designs have been developed adopting different types of greenhouse effect enclosure around one pot or one set of staggered pots, such as Cookit (SCI, 2020a), the Copenhagen Solar Cooker Light (SCI, 2020b), the Lightoven III (SCI, 2020c), the Haines 2.0 (SCI, 2021a), the HotPot (SCI, 2021b, Ebersviller and Jetter 2020) and the funnel concrete solar cooker as also known as Pucca cooker (Ruivo, 2017). Teong Tang (SCI, 2020d) developed some designs considering the possibility of no use of a transparent enclosure around the pot, such as the Foldable Fusion Cooker, Sun-Funnel, Fun-Panel, and the Suntastic Panel Cooker.

Several solar cookers have been investigated using a test procedure developed by Funk, 2000 for testing and reporting solar cooker performance (ASABE, 2013). Results of testing ten different designs of solar cookers have been reported by Solar Cookers International (SCI, 2020e) by evidencing that the standardised cooking power values obtained are in the range of 41 W to 117 W.

The two identical funnel cookers and the influence of the type of lid used in the pot, glass lid, or black metal lid have been investigated following the same protocol by Ruivo et al. 2021. The standardised cooker power obtained, for the funnel cooker, while using the glass lid (73.9 W) was clearly superior to that obtained while using the metal lid (50.6 W). The tests were performed during cold months under low sun elevation. The ratio of standardized cooking power to the solar radiation collecting area, while using the glass lid, is estimated to be 147.8 W/m<sup>2</sup>, which indicates that the performance of the funnel cooker is in between the performance of box-type cooker and parabolic-type cooker also tested recently by Ebersviller and Jetter, 2020. Chepkurui and Biira, 2020 tested four different sizes of the solar cooker with a funnel shape. Using the progression of water temperatures reported in this work, it is needed four hours to raise the temperature of 1 kg of water by 70 °C in the largest of the cookers, i.e., cooker with the biggest aperture area. Gupta et al., 2021 tested two different designs of low-cost reflective panel-type solar cooker vis-à-vis conventional box-type cooker. The test results show that the maximum temperature achieved by the load, i.e., water and rice for the best solar panel cooker, is around 70 °C. Thus, these cookers operate at very low temperatures.

The thermal performance of solar panel cookers mainly depends on meteorological conditions and different parameters such as the geometry and the aperture area of the cooker, the type and design of the cooking pot, the design of the greenhouse device adopted, and the quantity and type of food to be cooked. Thus, suitable-sized black painted or coated cooking pots with low weight and negligible wall thermal resistance are recommended. In most solar panel cookers designs, the cooking pots are wrapped with an appropriately sized transparent enclosure made of glass, acrylic, or plastic. Such enclosure provides a greenhouse effect and allows to retain heat and reduce the heat losses from the pot to the surrounding ambient. Despite the scarce data, like those indicated by Teong Tang (SCI, 2020d), evidences of such performance data are difficult to find in scientific literature.

Literature review depicts that the attainment of the desired cooking temperature for any solar cooker depends on the particular design of the cooker. Out of several designs of solar cookers, box-type designs are preferred for low-temperature cooking, wherein concentrating type and advance and modified designs are preferred for intermediate-temperature cooking.

However, solar panel cookers, particularly funnel cooker designs, are known to reach intermediate temperature, but there is a lack of information on this topic. Thus, it is interesting to check the realistic performance of solar panel cookers to attain temperatures in excess of the boiling temperature of the water. This may increase the acceptance of a low-cost and effective clean cooking solution by more users. Also, the modified and advanced designs of the solar panel cookers may be adopted for the households or the building with the limited sunny space for cooking.

Therefore, owing to the literature mentioned above gaps, the novelty and objectives of the present work are justified as i) to investigate the applicability of solar panel cooker to attain the temperatures above the boiling temperature of water for the first time, a subject of interest and research owing to their advantages mentioned above; ii) to test the applicability of suggested thermal performance parameter for solar panel cookers for the first time; iii) to evaluate solar panel cookers in terms of reference cooking time, maximum temperature attainment and inter-cooker performance comparison owing to small design change at intermediate temperatures using intermediate temperature test load because of lack of such comprehensive efforts, and iv) to comment on the

usefulness of solar panel cookers for intermediate temperature cooking and recommend their future prospective.

Therefore, the present work is initiated to investigate the performance of solar panel cookers with funnel configuration, usually called as solar funnel cookers, for the solar cooking at the intermediate temperature over the boiling point of water. Thus, for the first time, two identical designs of funnel cookers (Ruivo et al., 2021), named as FC1 and FC2, were tested using glycerine as a test load and Cooker Optothermal Ratio (COR) as a thermal performance parameter (Sagade et al., 2018b, 2019 and 2020; Tawfik et al., 2021). Cooker FC2 and FC1 were tested simultaneously with and without transparent glass enclosure on the cooking pot, respectively, under the same meteorological conditions. This allows the inter-cooker performance comparison of the cookers. Also, overall cooking efficiency ( $\eta$ ) is used to compare and comment on the performance of both cookers.

## 2. Materials and methods

### 2.1. Experimental setup and instrumentation

In the present work, the tests were carried out from October to December 2020. The experimental set-up was installed on the rooftop patio of the “Escuela de Ingenierías Industriales” at the University of Malaga in Spain (36.9° N, 4.4° W). The experimental setup is depicted in Fig. 1. The reflectors IPPON PANEL–LIGHT PE material and geometry maintained as it is depicted in Fig. 2. The distance between the two vertices A and B and the maximum value of the solar cooker aperture area of each reflector are 0.99 m and 0.5 m<sup>2</sup>, respectively. Each reflector has a reflective surface area of 1.063 m<sup>2</sup> and a reflectivity value, catalogued by the manufacturer, of 0.85. The design and construction of the cookers were described and detailed in the earlier study (Ruivo et al., 2021).

Only the modification made to the cookers in the present work was to put it on a support stand connected to a tripod as compared to a previous study (Ruivo et al., 2021). Also, the cookers were renamed as FC1 and FC2 instead of CSR1 and CSR2. Both the cookers were assembled to the tripod, with a stand at 38 cm above the floor of the patio, as depicted in Fig. 3. Both the cookers loaded with respective cooking sets were tested without being tilted, i.e., the line defined by points C and D, shown in Fig. 2, is parallel to the floor and the stand holding the cooking set.

Two identical cooking pots, made up of shiny black enameled carbon steel and equipped with identical glass lids, were used in the experiments. The cooking set without glass enclosure depicted in Fig. 4a was used in funnel cooker FC1, and the cooking set with glass enclosure shown in Fig. 4b is used in funnel cooker FC2.

Loading capacity of cooking pots is close to 3 L. The glass lids were made of tempered glass with a stainless-steel rim. The glass enclosure is composed of two transparent doors of washing machines. The inner volume of the glass enclosure is approximately 5.3 L, i.e., 77.5% greater

than the volume of the pot. Table 1 indicates the mass and specific heat values for the pots, lids, glass enclosure, and glycerine.

T-type thermocouples were used to measure the temperature of several points in each cooking set. Five of them were immersed in the glycerine at 10 mm from the bottom of the pot. An average value of the temperature of glycerine was determined and used in the calculations. A Campbell Scientific CR1000 data logger was used to record temperature readings every 15 s. The temperature instrumentation was described and detailed extensively in the previous study of Ruivo et al., 2021.

The solar irradiance was measured with two Hukseflux LP02 pyranometers, placed close to the cookers as shown in Fig. 4, and logged by the same data logger also every 15 s. One pyranometer was placed horizontally and the other on a tilted plane with an inclination angle of 50°. Using the measured irradiance values, beam normal irradiance and global normal irradiance were computed using the Liu Jordan sky model (Duffie and Beckman, 2013), with an albedo of 0.2. In the present experiments, the value of total solar radiation ( $G_T$ ) was measured normal to the beam radiation, and this corresponds to a maximum value of solar radiation recorded in that direction.

Also, wind speed ( $v$ ) and ambient air temperature ( $T_a$ ) were measured by a dedicated Onset weather station placed close to the cookers and logged with the same acquisition frequency adopted for solar irradiance and temperature at several positions of the cooking set.

During the experiments, azimuth adjustment of the cookers and the tilted pyranometer were performed simultaneously, every 20 min.

Another meteorological station at Engineering School's, which has a second data logger (Campbell Scientific CR1000) and pyranometers (Delta T Devices Ltd SPN1 and Hukseflux LP02), is placed near to the experimental setup. The data logged by this weather station was used to check and validate the measurements of the solar irradiance made by the station close to the cooker being tested.

### 2.2. Experimental methodology

In the present experiments, both cookers FC1 and FC2 were tested simultaneously side by side under the same weather conditions. The thermal performance of the cookers was estimated using thermal performance parameters, i.e., COR and  $\eta$  for the standard specific thermal load of 10.46 kJ/(m<sup>2</sup>C) defined by the ratio of the product of mass and heat specific of glycerine to the cooker maximum aperture area (Sagade et al., 2019). The thermal performance tests to determine the COR were performed using the test procedure reported by Sagade et al. 2018b.

Owing to the limitations of water as a standard test load (Sagade et al., 2018b), glycerine is preferred as a test. It enables performance investigation of cookers at a temperature higher than the boiling point of water. Moreover, glycerine as a test load allows better insight into the resolution of the thermal performance parameters as its specific heat is lower than that of water. Hence, it offers a higher resolution in design-

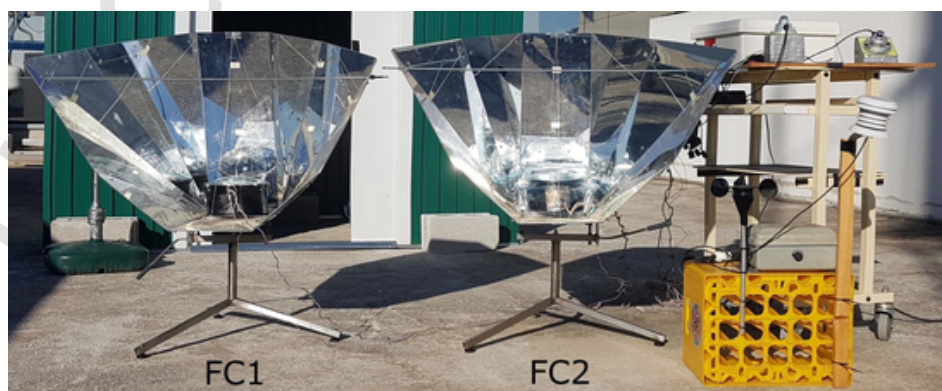


Fig. 1. Experimental test setup.

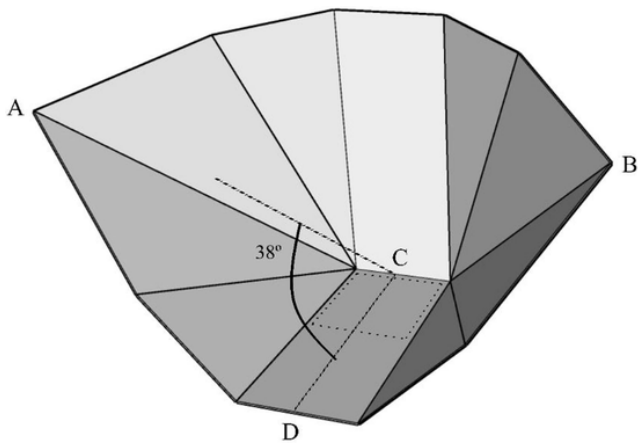


Fig. 2. Schematic design of the reflector of the funnel cooker.



Fig. 3. Funnel cooker assembled to the tripod with stand to hold the cooking set.

induced changes in thermal performance parameters. Thus, the rise in temperature per unit of heat gain is better visible. It enables the more realistic determination of thermal performance parameters for a specific design of solar cooker at low and intermediate-range of temperature (Sagade et al., 2018b).

In the present experiments, the solar cookers and the respective pots loaded with test load were heated near the ambient temperature before starting each experiment. This allows them to be in thermal equilibrium with the ambient. Then, both cookers were allowed to heat up under the solar radiation in the window of solar noon to allow the test load to attain an apparent stagnation temperature.

The experiments were conducted around 120 min of the local solar noon at the experimental location under the environmental conditions:  $G_T \geq 700 \text{ W/m}^2$ ;  $15 \text{ }^\circ\text{C} \leq T_a \leq 40 \text{ }^\circ\text{C}$  and  $v \leq 1.5 \text{ m/s}$ .

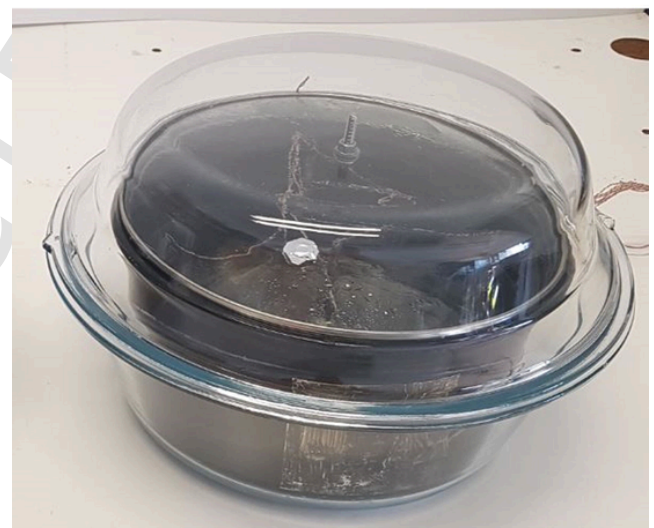
### 3. Thermal analysis of the solar funnel cookers

#### 3.1. Determination of the cooker Opto-thermal ratio

Several experimental tests were conducted to determine the thermal performance parameter Cooker Opto-thermal Ratio, COR, using the respective test procedure reported by Sagade et al., 2018b. The experimental measurements of heating tests were used to determine the value



a)



b)

Fig. 4. Cooking set: a) without a glass enclosure and b) with a glass enclosure.

Table 1  
Data for cooking set and glycerine.

	Metal pot	Glass lid	Glass enclosure	Glycerine
Mass (kg)	0.560	0.366	2.240	1.736
Specific heat (J/(kg°C))	510	670	Not applicable	3014

of the heat flux (Lahkar et al., 2012) that corresponds to the rate of useful heat gain by the test load per unit cooker aperture area ( $A_p$ ) as:

$$\dot{Q}'' = \frac{(M_f C_{pf})'_f (T_{f2} - T_{f1})}{A_p \Delta t} \quad (1)$$

where  $(M_f C_{pf})'_f$  is the sum of thermal capacitances of test load (glycerine) and the cooking pot along with lid;  $T_{f1}$  and  $T_{f2}$  are the fitted values

of initial and final temperatures of the test loads for a small interval  $\Delta t$ , respectively.

Using the measured experimental data for both the cookers, two characteristic curves of exponential fit of the temperature of the test load versus time and the corresponding linear fit of  $\frac{\dot{Q}''}{\bar{G}_T}$  vs.  $\frac{(T_{(gly)m} - \bar{T}_a)}{\bar{G}_T}$  were plotted. In the present case, glycerine was used as a test load. Thus,  $T_{fm}$  corresponds to  $T_{(gly)m}$ . The exponential relation is generated through a fit between the temperature of the test load and time. Here, the difference between fitted values of  $T_{f1}$  and  $T_{f2}$  for a small time interval  $\Delta t$  is used in Eq. (1) to calculate the  $\dot{Q}''$  value for that time interval and the mean of fitted values of  $T_{f1}$  and  $T_{f2}$  (i.e.,  $T_{fm}$ ) is used in the further analysis using the relevant plot for determination of COR (Sagade et al., 2020). For this, the corresponding linear fit of  $\frac{\dot{Q}''}{\bar{G}_T}$  vs.  $\frac{(T_{(gly)m} - \bar{T}_a)}{\bar{G}_T}$  is used to estimate  $F'\eta_o$  (intercept, i.e., optical efficiency factor) and  $F'U_i/C$  (symmetric value of the slope, with SI unit as  $W/(m^2 \text{ } ^\circ\text{C})$ ), which were used to determine the COR (Lahkar et al., 2012) by:

$$COR = \frac{F'\eta_o}{F'U_i/C} = \frac{\eta_o C}{U_i} \quad (2)$$

where,  $\eta_o$  is the optical efficiency,  $C$  is the concentration ratio and  $U_i$  is the heat loss factor.

### 3.2. Determination of overall cooker efficiency

The overall cooker efficiency ( $\eta$ ) is given by the ratio between the amount of solar energy transferred to the test load and the pot and the solar energy being collected by the cooker (Olwi and Khalifa, 1993; Harmim et al., 2012):

$$\eta = \frac{(M_f C_{pf})'_f \Delta T_f}{\bar{G}_T A_p \Delta t_{exp}} \quad (3)$$

where  $\Delta T_f$  is the difference between final and initial temperatures of test load for the entire duration of the experiment  $\Delta t_{exp}$ .

## 4. Results and discussion

Figs. 5a and 6a depict the rise in the temperature of glycerine in cookers FC2 and FC1, respectively, obtained in the experiment conducted on 10.11.2020. The corresponding linear plots of  $\frac{\dot{Q}''}{\bar{G}_T}$  vs.  $\frac{(T_{(gly)m} - \bar{T}_a)}{\bar{G}_T}$  are shown in Figs. 5b and 6b. Several experiments were conducted on different days to check the reproducibility of the results in terms of COR and overall cooker efficiency. The corresponding plots, the rise in the temperature of glycerine and  $\frac{\dot{Q}''}{\bar{G}_T}$  vs.  $\frac{(T_{(gly)m} - \bar{T}_a)}{\bar{G}_T}$  are presented in Appendix A.

As expected, the rate of the temperature rise of test load decreases with an increase in time. When it becomes very low near the end of the window of 4 h of solar noon, an apparent stagnation temperature is reached, depending upon the ambient conditions of a location and the design of the solar cooker (see Figs. 5a, 6a, and Figs. A1a to A14a).

In the case of FC1, the typical value of the apparent stagnation temperature attained by glycerine ( $T_{g,st}$ ) is seen to be  $116.2 \text{ } ^\circ\text{C}$ , and that value for FC2 is seen to be  $146.1 \text{ } ^\circ\text{C}$ , respectively, on the given experimental day at a location. A seasonal variation is expected to occur in the apparent stagnation temperature ( $T_{g,st}$ ). It is evident that there is a gradual fall in solar irradiance after attaining the highest value around the solar noon. In the case of cooker FC2, it is seen that the glass enclosure is adequate to speed up the heating process and maintain the temperature of the test load as compared to cooker FC1 without a glass enclosure.

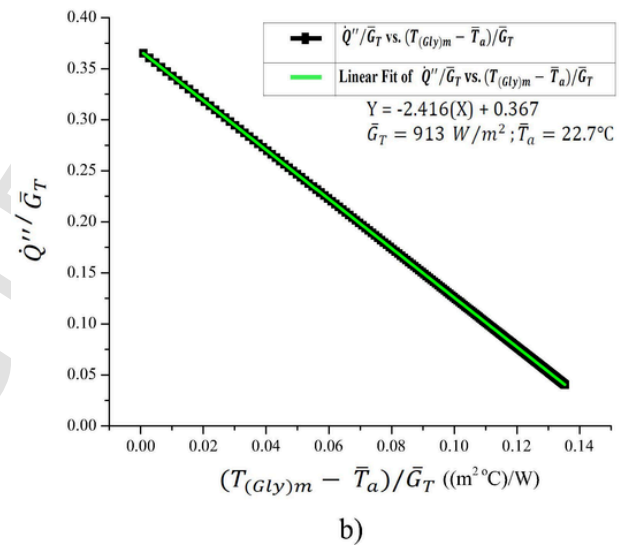
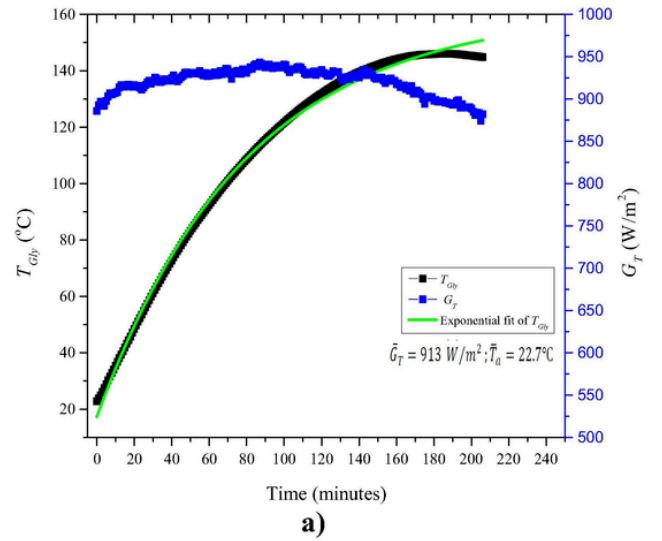


Fig. 5. Characteristic plots of cooker FC2 on test day 10.11.2020: a) temperature of glycerine ( $T_{gly}$ ) and solar irradiance vs. time and b) Linear fit of  $\frac{\dot{Q}''}{\bar{G}_T}$  vs.  $\frac{(T_{(gly)m} - \bar{T}_a)}{\bar{G}_T}$ .

Also, the use of the cooking set with a glass enclosure may enhance the time constant of FC2 as compared to FC1. It may be one reason for the delayed response of cooker FC2 to the fall in the value of the temperature of glycerine associated with the decline in solar irradiance. Thus, using cooking set with a glass enclosure influences the possible attainment of a comparatively high value of apparent stagnation temperature of glycerine with FC2 than FC1.

The values of  $F'\eta_o$  and  $F'U_i/C$  determined from the respective linear plots of  $\frac{\dot{Q}''}{\bar{G}_T}$  vs.  $\frac{(T_{(gly)m} - \bar{T}_a)}{\bar{G}_T}$  for both cookers, FC1 and FC2, along with their mean values, are listed in Table 2. It is observed that the mean values  $F'\eta_o$  and  $F'U_i/C$  for FC2 are seen to be  $0.301 \pm 0.049$  and  $1.922 \pm 0.387$ , respectively, with a percentage standard deviation of 16.6% and 20%, respectively. Similarly, the mean values of  $F'\eta_o$  and  $F'U_i/C$  for FC1 are estimated to be  $0.299 \pm 0.056$  and  $2.730 \pm 0.560$  respectively, with a percentage standard deviation of 18.7% and 20.5%, respectively.

Subsequently, the mean values of the COR for the cookers FC1 and FC2 are determined to be  $0.157 \pm 0.008 \text{ (m}^2\text{ } ^\circ\text{C)/W}$  and  $0.110 \pm 0.006$

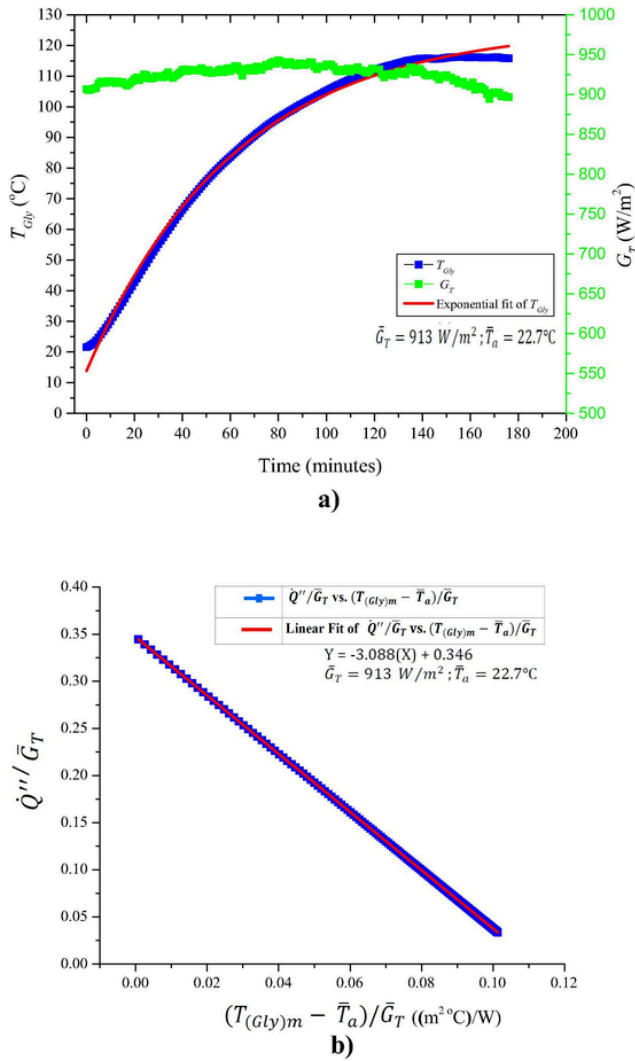


Fig. 6. Characteristic plots of cooker FC1 on test day 10.11.2020: a) temperature of glycerine ( $T_{Gly}$ ) and solar irradiance vs. time and b) linear fit of  $\frac{Q''}{G_T}$  vs.  $\frac{(T_{Gly,m} - \bar{T}_a)}{G_T}$ .

( $m^2C$ )/W, respectively. A percentage standard deviation in the mean values of COR of the cookers FC1 and FC2 are seen to be approximately 5.1% and 5.45%, respectively. From the experimental results, it can be seen that the mean value of COR for a particular design of solar cooker, either FC1 or FC2, remains approximately unchanged with acceptable deviations. Also, the literature results (Lahkar et al., 2012; Sagade et

Table 2  
Summary of the experimental data and performance parameters of solar cookers.

Test day	Test conditions	Performance parameters of cooker FC2					Performance parameters of cooker FC1		
		Solar altitude angle at noon (°)	$\bar{G}_T$ ( $W/m^2$ )	$\bar{T}_a$ (°C)	$F'\eta_o$	$F'U_i/C$ ( $W/(m^2C)$ )	COR ( $m^2C/W$ )	$F'\eta_o$	$F'U_i/C$ ( $W/(m^2C)$ )
27.10.2020	40.3	960	24.4	0.359	2.298	0.156	0.394	3.539	0.111
30.10.2020	39.3	938	22.8	0.345	2.358	0.146	0.337	3.336	0.101
10.11.2020	36.0	913	22.7	0.367	2.416	0.152	0.346	3.088	0.112
17.11.2020	34.2	920	22.1	0.290	1.891	0.153	0.290	2.837	0.102
20.11.2020	33.5	895	22.4	0.289	1.769	0.164	0.288	2.532	0.114
2.12.2020	31.2	951	21.2	0.257	1.682	0.153	0.255	2.382	0.107
9.12.2020	30.4	881	15.3	0.261	1.590	0.164	0.242	2.118	0.114
18.12.2020	29.9	871	17.8	0.238	1.392	0.171	0.237	2.006	0.118
Mean value with standard deviation				0.301 ± 0.049	1.925 ± 0.387	0.157 ± 0.008	0.299 ± 0.056	2.730 ± 0.560	0.110 ± 0.006
Percentage standard deviation				16.6%	20.1%	5.1%	18.7%	20.5%	5.45%

al., 2018; Sagade et al., 2019; Sagade et al., 2020; Khallaf et al., 2020) confirm the same. Table 2 depicts the results achieved for both cookers FC2 and FC1.

#### 4.1. Determination of COR dependent objective parameters

Theoretical values of COR dependent objective parameters, maximum achievable fluid temperature ( $T_{fmax}$ ), and reference time ( $\tau_R$ ) for both the funnel cookers were determined using the value of COR on a given experimental day. Objective parameters are dependent on the meteorological conditions of a location on a typical experimental day, and seasonal variations are expected in their values (Sagade et al., 2020).

The theoretical value of  $T_{fmax}$  on a typical experimental day can be determined (Lahkar and Samdarshi, 2010 and Lahkar et al., 2012) by:

$$T_{fmax} = \bar{T}_a + COR(\bar{G}_T) \quad (4)$$

The reference time ( $\tau_R$ ) is a theoretical time taken by the test load to heat up from lower to the upper limit of temperature under given meteorological conditions. It can be determined (Lahkar et al., 2012; Sagade et al., 2018) by:

$$\tau_R = \frac{(M_f C_{pf})'_f}{A_p F' \eta_o} \times COR \times \ln \left[ \frac{\bar{G}_T - \frac{T_{f1} - \bar{T}_a}{COR}}{\bar{G}_T - \frac{T_{f2} - \bar{T}_a}{COR}} \right] \quad (5)$$

In the case of FC2, the typical maximum and minimum theoretical values of  $T_{fmax}$  and  $\tau_R$  are estimated to be 174.2 °C and 159.8 °C, respectively, and 37.4 min and 63.4 min, respectively. Similarly, in the case of FC1, the typical maximum and minimum theoretical values of  $T_{fmax}$  and  $\tau_R$  are estimated to be 131.3 °C and 116.1 °C, respectively, and 43.6 min and 96.4 min, respectively. On the other hand, experimentally observed maximum and minimum values of the  $T_{fmax}$  and  $\tau_R$  for FC2 are 154.5 °C and 123.1 °C, respectively and 38 min and 61 min, respectively, and that for FC1 are seen to be 125.4 °C and 98.1 °C, respectively and 43 min and 89 min, respectively.

Table 3 depicts the comparison of the theoretical and experimental values of the two objective parameters for both the cookers.

Comparing the theoretical and experimental values of both objective parameters depicts that the FC2 performs better than FC1. The improvement in the performance of the FC2 can be attributed to the glass enclosures, which produce the greenhouse effect. More details are discussed in the upcoming section 4.2.

#### 4.2. Comparison of inter-cooker performance of cookers FC1 and FC2

The results of experiments of two identical designs of funnel cookers FC1 and FC2 are compared to comment on the inter-cooker perfor-

**Table 3**  
Theoretical and experimental values of the objective parameters for cookers FC1 and FC2.

Test Day	Test conditions		Cooker FC2 values				Cooker FC1 values					
	$\bar{T}_a$ (°C)	$\bar{G}_T$ (W/m <sup>2</sup> )	COR (m <sup>2</sup> C/W)	Theoretical		Experimental		COR (m <sup>2</sup> C/W)	Theoretical		Experimental	
				$T_{fmax}$ (°C)	$\tau_R$ (min)	$T_{fmax}$ (°C)	$\tau_R$ (min)		$T_{fmax}$ (°C)	$\tau_R$ (min)	$T_{fmax}$ (°C)	$\tau_R$ (min)
27.10.2020	24.4	960	0.156	174.2	37.4	154.5	38	0.111	131.3	43.6	125.4	43
30.10.2020	22.8	938	0.146	160.0	42.6	148.4	43	0.101	117.6	62.8	111.6	56
10.11.2020	22.7	913	0.152	161.5	40.9	146.1	42	0.112	125.0	56.7	116.1	52
17.11.2020	22.1	920	0.153	162.6	51.5	137.2	51	0.102	116.1	76.8	105.2	70
20.11.2020	22.4	895	0.164	168.9	51.4	142.6	50	0.114	124.2	70.4	112.9	65
02.12.2020	21.2	951	0.153	166.3	55.6	140.2	54	0.107	123.0	76.9	110.9	69
09.12.2020	15.3	919	0.164	159.8	63.4	123.1	56	0.114	120.3	92.2	98.1	89
18.12.2020	17.8	871	0.171	166.8	66.8	133.4	61	0.118	120.7	96.4	102.9	86

mance. The values of different experimentally determined parameters are used to reach the conclusions.

It is seen that FC2 is able to attain a higher apparent stagnation temperature as compared to FC1. Figs. 5a and 6a depict that the rise in the temperature of the test load is fast, and the attainment of apparent stagnation temperature of glycerine is seen to be higher in the case of FC2 as compared to FC1. It enhances the reference time of the FC2 as compared to FC1.

The mean value of  $F'U_l/C$  for cooker FC2 is lower than that for FC1 as expected (see Table 2). It can be attributed to the use of the glass enclosure in cooker FC2 that enables the trapping and retaining of heat. Also, it leads to the attainment of a relatively high apparent stagnation temperature in FC2 as compared to FC1. This may be due to the property of glass, which blocks the longer wavelength re-radiation from the glass enclosure and gets heat up. Moreover, the glass enclosure decreases the convective losses from the cooking pot of FC2 as well. On the other hand, the cooking pot of FC1 is exposed directly to ambient and may be responsible for the increase in the heat losses compared to FC2. Thus, the mean values of the  $F'U_l/C$  are seen to be lowered in cooker FC2 as compared to cooker FC1.

Contrary to the expectation, the mean value of  $F'\eta_0$  for FC2 is seen to be approximately equal to FC1. It can be attributed to the property of glass to transmit the shorter wavelength solar radiation to the cooking pot of FC2.

Also, cooking pots in both cookers may not be able to absorb a complete range of the solar spectrum, which may impact the optical performance of cooking pots. This may result in an approximately equal value of the optical efficiency factor for cookers, FC1 and FC2. But, the lower value of the  $F'U_l/C$  in the case of FC2 more than compensates any reduction in the value of  $F'\eta_0$ .

Thus, the use of a glass enclosure on the cooking set of FC2 leads to a positive impact on the COR's value. Hence, the mean value of COR for the FC2 is seen to be improved as compared to FC1.

From the comparison of the two objective parameters given in Table 3, it can be seen that typical experimental values of the maximum achievable fluid temperature and of reference time are seen to be improved for FC2 as compared to the typical experimental values attained with FC1. The performance increment can be attributed to a relatively lower mean value of the  $F'U_l/C$ , which is clearly visible for FC2. However,  $F'\eta_0$  may have a negligible effect on the performance of the cooker in comparison to  $F'U_l/C$ .

As shown in Table 3, the mean value of the COR for FC2 is improved compared to FC1. Hence, COR seems to be sufficient to reflect design interventions in the solar cooker and precisely predict the inter-cooker performance comparison with reasonable accuracy.

Thus, from the experimental results, it can be concluded that the use of a glass enclosure on the cooking pot of FC2 helps to enhance the opto-thermal performance of the cooker in terms of reference time.

Glass enclosure not only helps in attaining a relatively higher temperature in case of FC2, but also enables a fast-heating process of the

load compared to FC1. Also, the glass enclosure improves the heat retention ability of the FC2.

#### 4.3. Overall efficiency of the funnel cookers

The overall cooker efficiency values for both the cookers FC1 and FC2 are determined by using Eq. (3) for each experiment on a typical day. The calculated average values of  $\eta$  are 11.8% and 10.2% for FC2 and FC1, respectively. Thus, it clearly depicts that the FC2 performs better as compared to FC1. Also, the overall cooker efficiency obtained for both cookers is compared with the cookers reported in the literature. Results show that efficiencies of cookers FC1 and FC2 are reasonably improved as compared to that reported by Olwi and Khalifa (1993) and Harmim et al. (2012).

However, it is essential to note that test load, glycerin, is able to attain temperature values greater than the boiling point of water. Moreover, overall thermal resistance to the heat transfer between test load and ambient is more significant in the case of FC2 as compared to FC1. Thus, FC2 may have lower values of thermal losses as compared to FC1. However, both solar funnel cookers work with low concentration ratios and may have low optical efficiency. This may result in lower overall cooker efficiency for both cookers. However, the overall efficiency of cooker FC2 is slightly higher than FC1 because the cooker FC2 was tested using the glass enclosure on the cooking pot. This glass enclosure acts as a heat trap. It reduces the heat losses from the cooking pot, improving the performance of the cooker FC2, which is reflected in terms of the relatively high value of overall cooker efficiency for the cooker FC2 than cooker FC1. Therefore, these results of funnel cookers are encouraging for future improvements.

## 5. Conclusions

The present work discusses the possible application of solar funnel cookers attaining an intermediate temperature cooking greater than the boiling point of water. The thermal performance of solar cookers is estimated using COR and overall cooker efficiency. Also, the inter-cooker performance of the cookers FC1 and FC2 are compared based on COR-dependent objective parameters to comment on the performance of cookers at intermediate temperature. The major finding of the present work are as follows:

- i) Experimental results clearly depict that solar funnel cookers are able to attain temperatures in the range of 140 to 150 °C with the use of the glass enclosure.
- ii) The mean values of COR for the FC2 and FC1, using glycerine as a test load, are estimated to be 0.157 m<sup>2</sup>C/W and 0.110 m<sup>2</sup>C/W, respectively. Also, the average values of overall cooker efficiency are 11.8% and 10.2% for FC2 and FC1, respectively.
- iii) Based on the values of COR and overall cooker efficiency, it is concluded that FC2 performs better as compared to FC1. The glass

enclosure on the cooking pot in the case of FC2 imparts the greenhouse effect and helps to enhance the opto-thermal performance of the cooker. It enables to improve the reference time, providing faster heating of the load as compared to FC1. It also helps in attaining relatively high values of the apparent stagnation temperature in the case of FC2 compared to FC1. Also, glass enclosure enables reduces the heat losses from cooker FC2 may improve the cooker's heat retention ability.

- iv) The overall efficiency of cooker FC1 is slightly lower than FC2. A glass enclosure used in the cooker FC2 helps to reduce the heat losses from the cooking pot. This leads to improving the thermal performance of the cooker FC2 than FC1.
- v) The typical experimental values of reference cooking time for cooker FC1 and FC2 are 43 min and 38 min, respectively. The typical experimental values of maximum achievable load temperature for FC1 and FC2 are 125.4 °C and 154.5 °C, respectively. This clearly shows that solar panel cookers can attain temperatures in excess of the boiling temperature of the water. They help cook the boiling type of food and intermediate-temperature food items. Also, as expected, they can cook faster under clear sun conditions. Thus, solar panel cookers can be vital devices in the propagation of clean cooking technologies.
- vi) Presented results for solar funnel cookers are unique and encouraging, owing to their different advantages. Thus, they can be utilized for future developments, such as a) investigation of different tracking reflector designs, b) investigation of possibilities of incorporating additional heat storage elements, and c) investigation of cookers performance under high solar altitude angles. Such developments may improve the designs of relatively simple configurations of the funnel cookers, and they may be able to perform better.

- vii) Thus, the experimental results of the present solar funnel cooker may be necessary for the propagation of the solar cooking technology to the common people.

#### Uncited references

Lahkar and Samdarshi, 2010; Mullick et al., 1987.

#### CRediT authorship contribution statement

**Xabier Apaolaza-Pagoaga:** Conceptualization, Methodology, Formal analysis, Investigation, Data curation, Visualization, Writing – review & editing. **Atul A. Sagade:** Conceptualization, Methodology, Supervision. **Celestino Rodrigues Ruivo:** Conceptualization, Methodology, Investigation, Formal analysis, Writing – original draft. **Antonio Carrillo-Andrés:** Software, Data curation.

#### Declaration of Competing Interest

The authors declare that they have no known competing financial interests or personal relationships that could have appeared to influence the work reported in this paper.

#### Acknowledgements

Atul A. Sagade acknowledges the research funding support of *Solar Energy Research Center (SERC), Chile FONDAP/ANID grant number 15110019*.

## Appendix A.

### A.1. Reproducibility of the results

Figs. 5 and 6 show the characteristic plots for one experiment of testing cookers FC2 and FC1, respectively. In this appendix, the same characteristic plots are presented for the experiments performed on different days. Figs. A1–A7 show the characteristic plots for cooker FC2 and Figs. A8–A14 show the plots for cooker FC1.

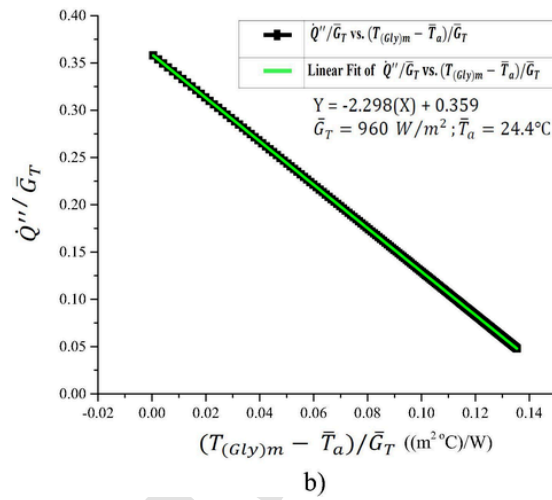
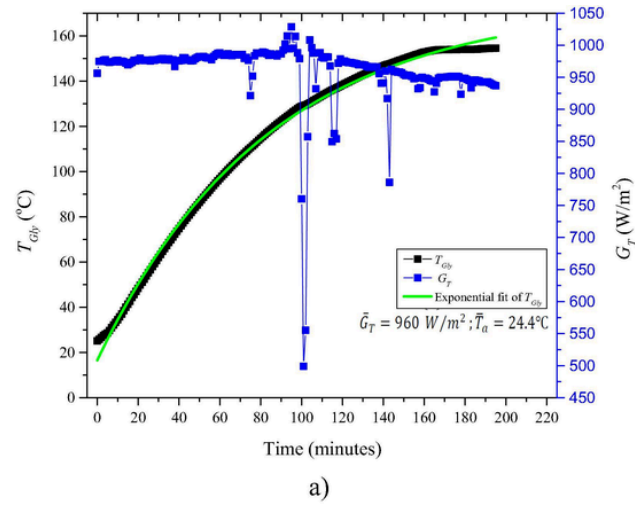


**Fig. A1.** Characteristic plots of cooker FC2 on test day 27.10.2020: a) temperature of glycerine ( $T_{Gly}$ ) and solar irradiance vs. time and b) linear fit of  $\frac{Q''}{G_T}$  vs.  $\frac{(T_{Gly})_m - \bar{T}_a}{G_T}$ .

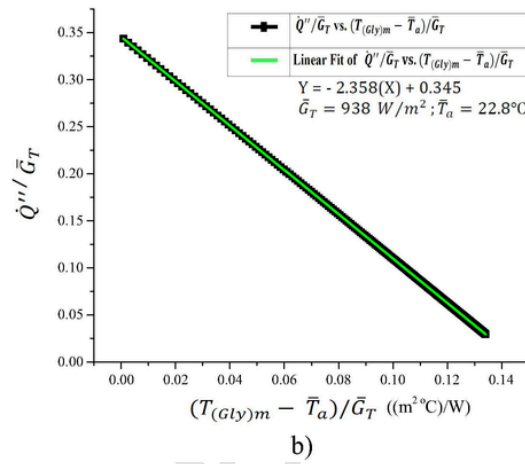
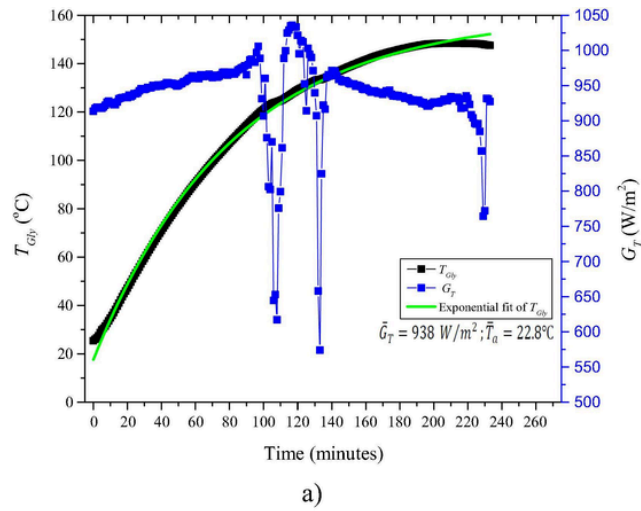
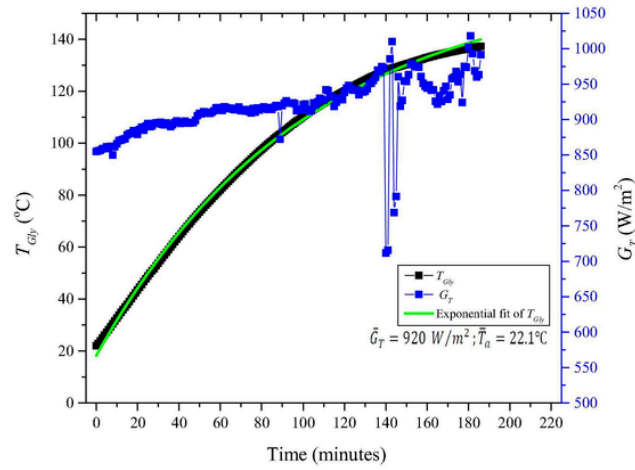
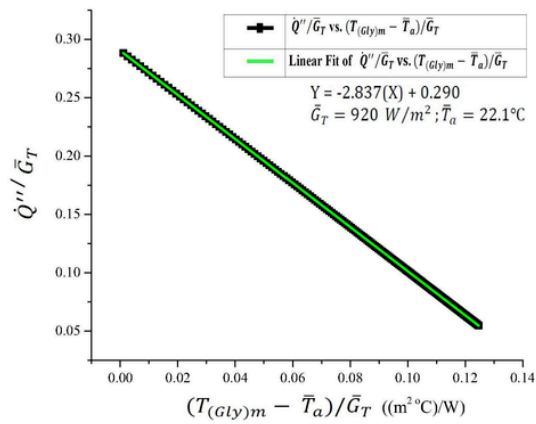


Fig. A2. Characteristic plots of cooker FC2 on test day 30.10.2020: a) temperature of glycerine ( $T_{gly}$ ) and solar irradiance vs. time and b) linear fit of  $\frac{Q''}{G_T}$  vs.  $\frac{(T_{gly,m} - \bar{T}_a)}{\bar{G}_T}$ .



a)



b)

**Fig. A3.** Characteristic plots of cooker FC2 on test day 17.11.2020: a) temperature of glycerine ( $T_{gly}$ ) and solar irradiance vs. time and b) linear fit of  $\frac{Q''}{G_T}$  vs.  $\frac{(T_{gly,m} - \bar{T}_a)}{G_T}$ .

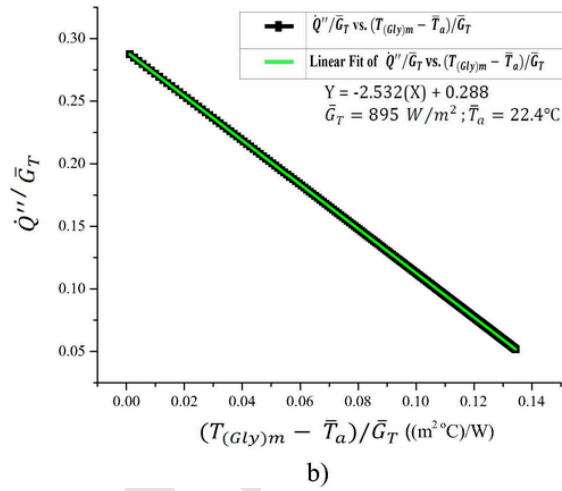
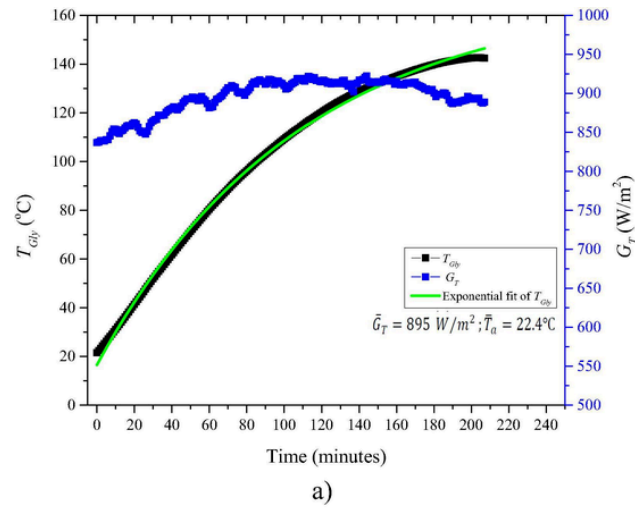


Fig. A4. Characteristic plots of cooker FC2 on test day 20.11.2020: a) temperature of glycerine ( $T_{gly}$ ) and solar irradiance vs. time and b) linear fit of  $\frac{Q''}{G_T}$  vs.  $\frac{(T_{gly,m} - \bar{T}_a)}{G_T}$

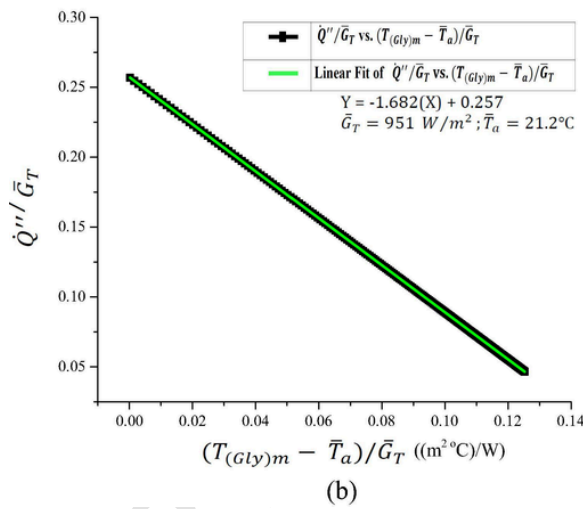
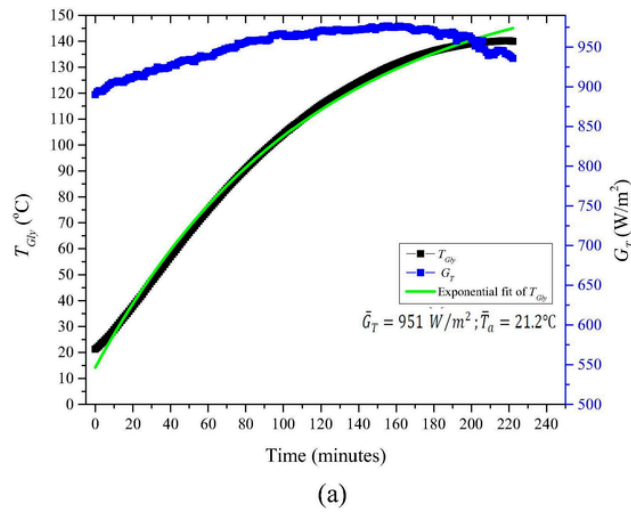
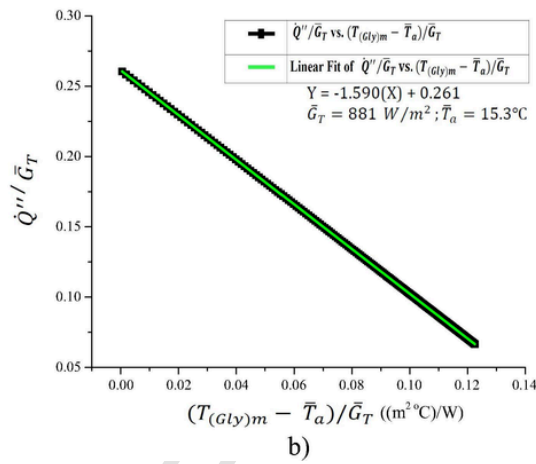
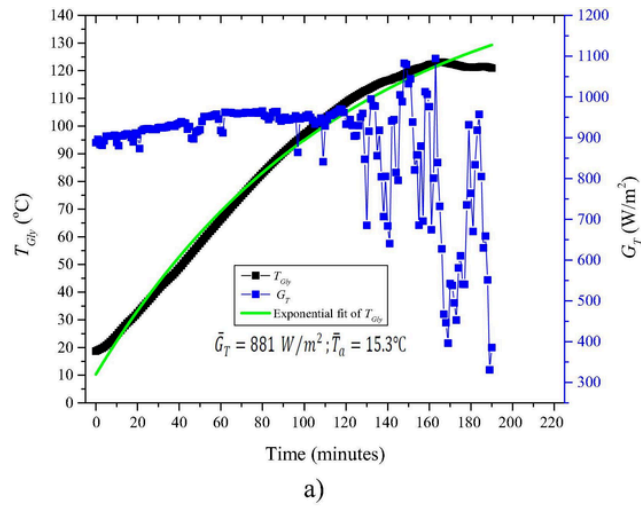
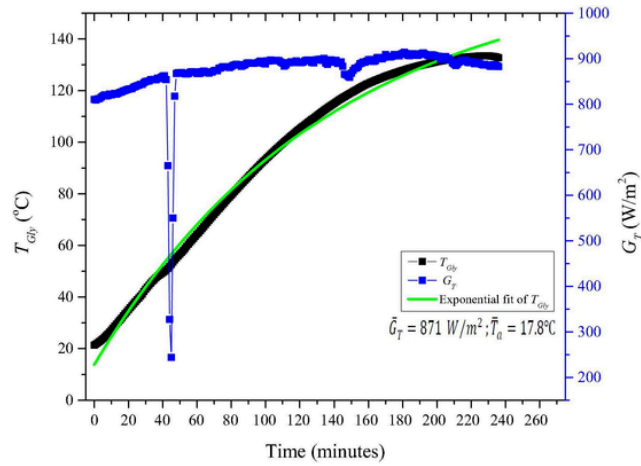


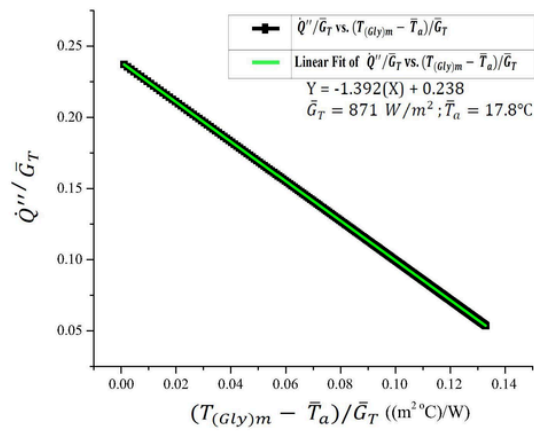
Fig. A5. Characteristic plots of cooker FC2 on test day 2.12.2020: a) temperature of glycerine ( $T_{Gly}$ ) and solar irradiance vs. time and b) linear fit of  $\frac{Q''}{G_T}$  vs.  $\frac{(T_{Gly})_m - \bar{T}_a}{G_T}$ .



**Fig. A6.** Characteristic plots of cooker FC2 on test day 09.12.2020: a) temperature of glycerine ( $T_{gly}$ ) and solar irradiance vs. time and b) linear fit of  $\frac{dT_{gly}}{dt}$  vs.  $\frac{(T_{gly,m} - \bar{T}_a)}{\bar{G}_T}$ .



a)



b)

**Fig. A7.** Characteristic plots of cooker FC2 on test day 18.12.2020: a) temperature of glycerine ( $T_{gly}$ ) and solar irradiance vs. time and b) Linear fit of  $\frac{\dot{Q}''}{\bar{G}_T}$  vs.  $\frac{(T_{gly})_m - \bar{T}_a}{\bar{G}_T}$ .

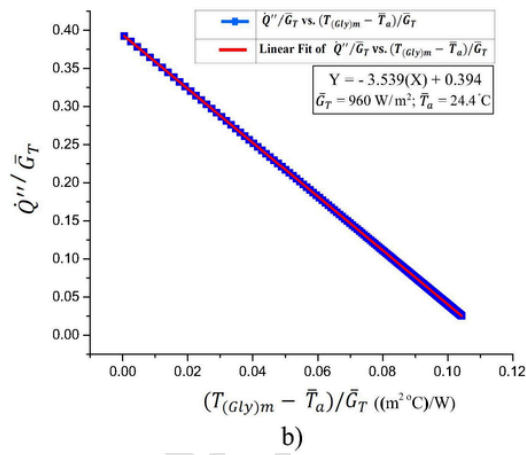
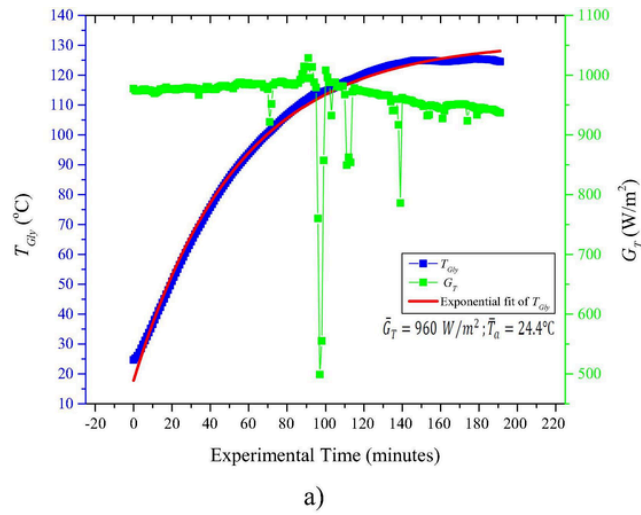


Fig. A8. Characteristic plots of cooker FC1 on test day 27.10.2020: a) temperature of glycerine ( $T_{gly}$ ) and solar irradiance vs. time and b) linear fit of  $\frac{Q''}{G_T}$  vs.  $\frac{(T_{gly})_m - \bar{T}_a}{\bar{G}_T}$ .

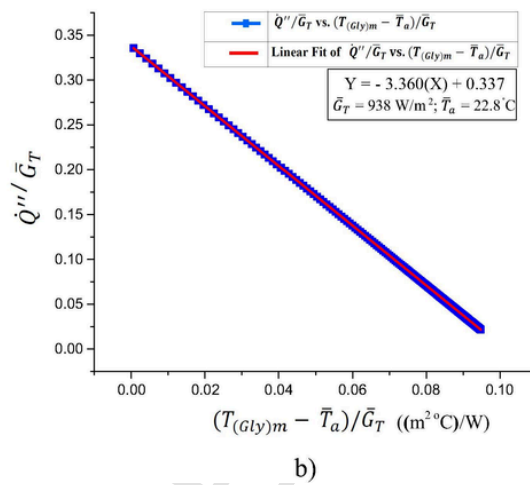
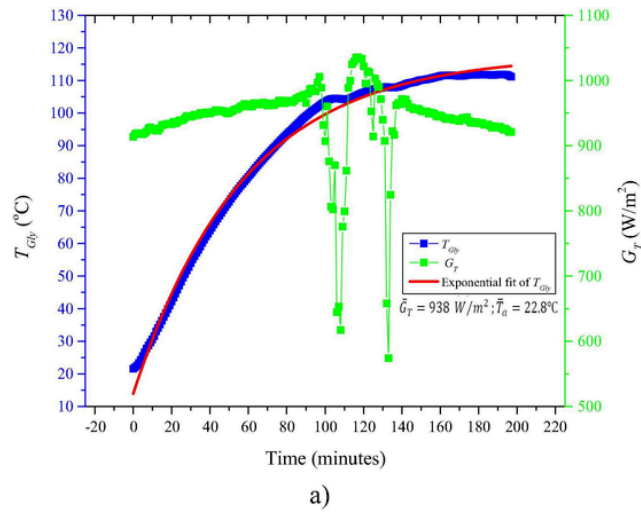
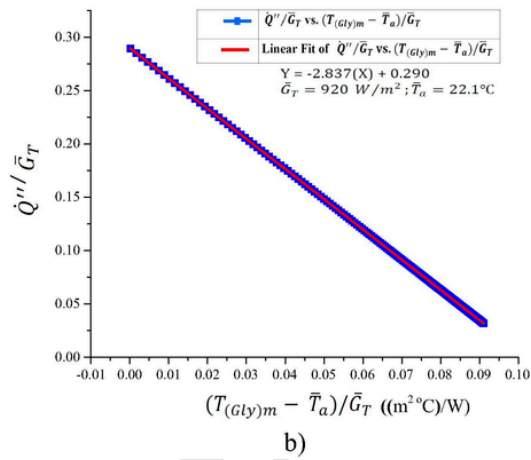
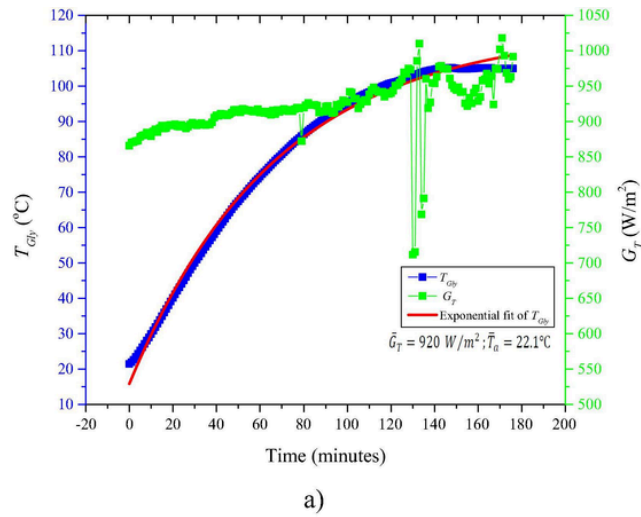
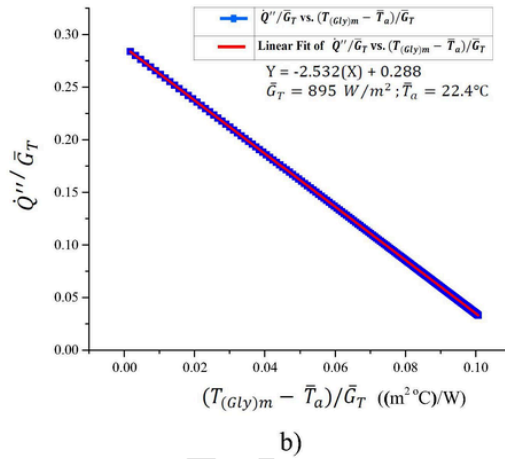
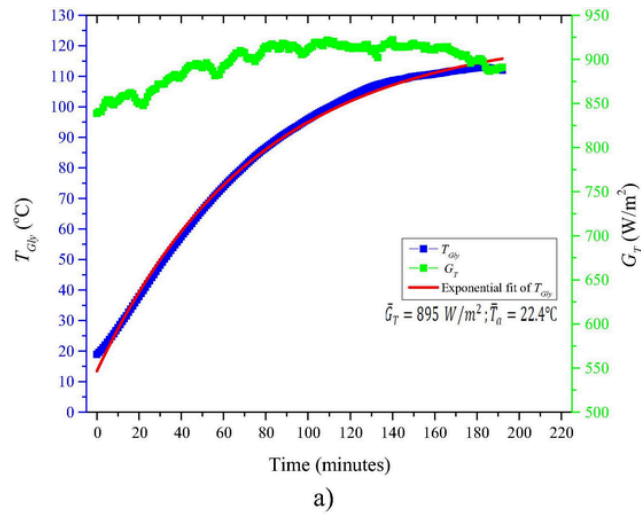


Fig. A9. Characteristic plots of cooker FC1 on test day 30.10.2020: a) temperature of glycerine ( $T_{gly}$ ) and solar irradiance vs. time and b) linear fit of  $\frac{Q''}{G_T}$  vs.  $\frac{(T_{gly})_m - \bar{T}_a}{G_T}$ .



**Fig. A10.** Characteristic plots of cooker FC1 on test day 17.11.2020: a) temperature of glycerine ( $T_{gly}$ ) and solar irradiance vs. time and b) linear fit of  $\frac{\dot{Q}''}{G_T}$  vs.  $\frac{(T_{(gly)m} - \bar{T}_a)}{G_T}$ .



**Fig. A11.** Characteristic plots of cooker FC1 on test day 20.11.2020: a) temperature of glycerine ( $T_{gly}$ ) and solar irradiance vs. time and b) linear fit of  $\frac{Q''}{G_T}$  vs.  $\frac{(T_{gly)m} - \bar{T}_a)}{G_T}$ .

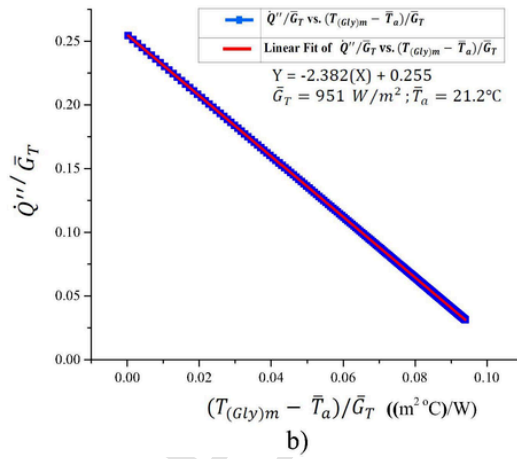
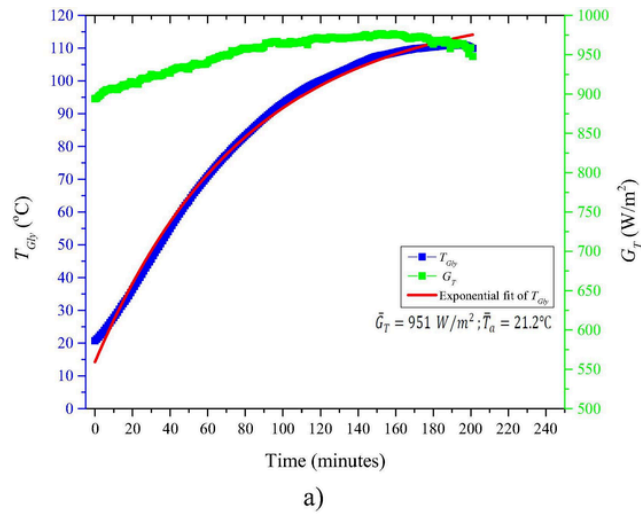


**Fig. A12.** Characteristic plots of cooker FC1 on test day 2.12.2020: a) temperature of glycerine ( $T_{gly}$ ) and solar irradiance vs. time and b) linear fit of  $\frac{Q''}{G_T}$  vs.  $\frac{(T_{gly})_m - \bar{T}_a}{\bar{G}_T}$ .

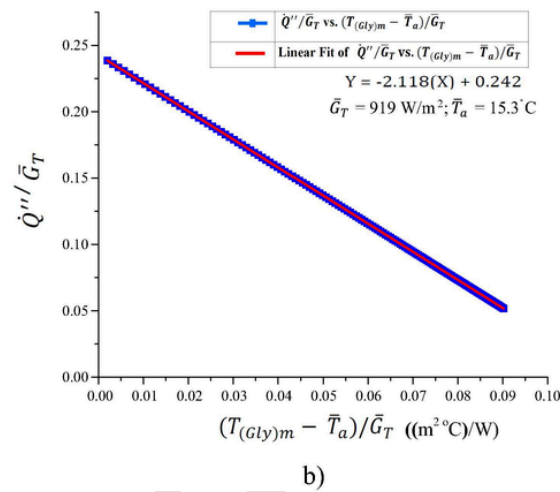
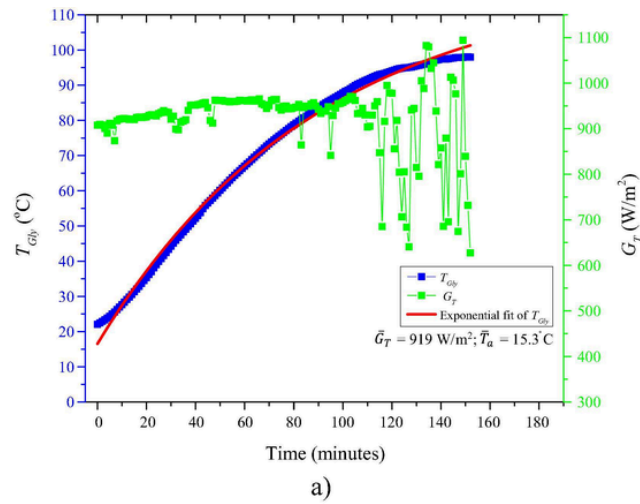


**Fig. A13.** Characteristic plots of cooker FC1 on test day 9.12.2020: a) temperature of glycerine ( $T_{Gly}$ ) and solar irradiance vs. time and b) linear fit of  $\frac{Q''}{G_T}$  vs.  $\frac{(T_{Gly})_m - \bar{T}_a}{G_T}$ .

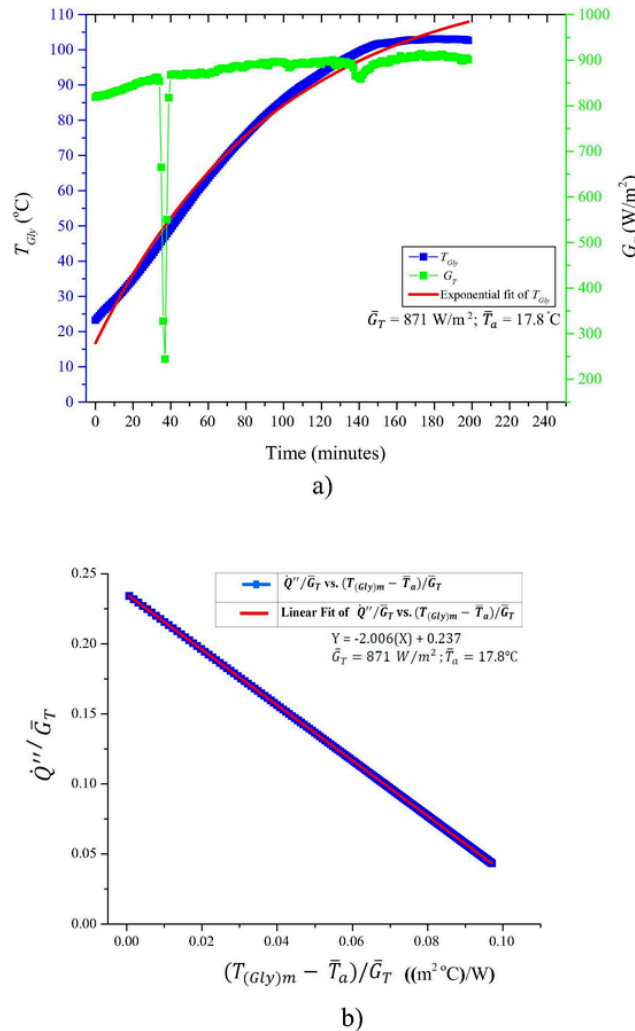


Fig. 14. Characteristic plots of cooker FC1 on test day 18.12.2020: a) temperature of glycerine ( $T_{gly}$ ) and solar irradiance vs. time and b) linear fit of  $\frac{\dot{Q}''}{\bar{G}_T}$  vs.  $\frac{(T_{(gly)m} - \bar{T}_a)}{\bar{G}_T}$ .

References

Abd-Elhady, M.S., Abd-Elkerim, A.N.A., Ahmed, S., Halim, M.A., Okail, A.I., 2019. Study the thermal performance of solar cookers by using metallic wires and nanographene. *Renew. Energy* 153, 108–116. <https://doi.org/10.1016/j.renene.2019.09.037>.

Algifri, A.H., Al-Towaie, H.A., 2001. Efficient orientation impacts of box-type solar cooker on the cooker performance. *Sol. Energy* 70 (2), 165–170. [https://doi.org/10.1016/S0038-092X\(00\)00136-5](https://doi.org/10.1016/S0038-092X(00)00136-5).

Anilkumar, B., Maniyeri, R., Anish, S., 2020. Design, fabrication and performance assessment of a solar cooker with optimum composition of heat storage materials. *Environ. Sci. Pollut. Res.* <https://doi.org/10.1007/s11356-020-11024-3>

Arif, R.M., Khan, A.M., Azhar, M., Akhtar, N., Meraj, M., 2021. Thermal performance comparison and augmentation of two identical box-type solar cookers operating in tropical climatic conditions. *J. Thermal Sci. Eng. Appl.* 13 (6), 061004. <https://doi.org/10.1115/1.4050323>.

ASABE, 2013. ASAE S580.1 NOV2013, Testing and Reporting Solar Cooker Performance. American Society of Agricultural and Biological Engineers, St. Joseph, Michigan, USA.

Balzar, A., Stumpf, P., Eckhoff, S., Ackermann, H., Grupp, M., 1996. A solar cooker using vacuum-tube collectors with integrated heat pipes. *Sol. Energy* 58 (1–3), 63–68. [https://doi.org/10.1016/0038-092X\(96\)00024-2](https://doi.org/10.1016/0038-092X(96)00024-2).

Chepkurui, J., Biira, S., 2020. Thermal performance evaluation of the funnel solar cooker of different funnel lengths implemented in Nagongera. *Uganda. Tanz. J. Sci.* 46, 53–60.

Coccia, G., Aquilanti, A., Tomassetti, S., Comodi, G., Di Nicola, G., 2020. Design, realization, and tests of a portable solar box cooker coupled with an erythritol-based PCM thermal energy storage. *Sol. Energy* 201, 530–540. <https://doi.org/10.1016/j.solener.2020.03.031>.

Coccia, G., Di Nicola, G., Pierantozzi, M., Tomassetti, S., Aquilanti, A., 2017. Design, manufacturing, and test of a high concentration ratio solar box cooker with multiple reflectors. *Sol. Energy* 155, 781–792. <https://doi.org/10.1016/j.solener.2017.07.020>.

Craig, O.O., Dobson, R.T., 2017. A novel indirect parabolic solar cooker. *J. Electr. Eng.* 5, 137–142. <https://doi.org/10.17265/2328-2223/2017.03.003>.

Cuce, P.M., Kolayli, S., Cuce, E., 2020. Enhanced performance figures of solar cookers through latent heat storage and low-cost booster reflectors. *Int. J. Low – Carbon Technol.* 15 (3), 427–433. <https://doi.org/10.1093/ijlct/ctz079>.

Cuce, P.M., 2018. Box type solar cookers with sensible thermal energy storage medium: A comparative experimental investigation and thermodynamic analysis. *Sol. Energy* 166, 432–440. <https://doi.org/10.1016/j.solener.2018.03.077>.

Duffie, J.A., Beckman, W.A. 2013. *Solar Engineering of Thermal Processes*, fourth ed., Wiley.

Ebersviller, S.M., Jetter, J.J., 2020. Evaluation of performance of household solar cookers. *Sol. Energy* 208, 166–172. <https://doi.org/10.1016/j.solener.2020.07.056>.

Edmonds, I., 2018. Low cost realisation of a high temperature solar cooker.. *Renewable Energy* 121, 94–101. <https://doi.org/https://doi.org/10.1016/j.renene.2018.01.010>.

El-Sebah, A., 1997. Thermal performance of a box-type solar cooker with outer-inner reflectors. *Energy* 22 (10), 969–978. [https://doi.org/10.1016/S0360-5442\(97\)00027-3](https://doi.org/10.1016/S0360-5442(97)00027-3).

Esen, M., 2004. Thermal performance of a solar cooker integrated vacuum-tube collector with heat pipes containing different refrigerants. *Sol. Energy* 76 (6), 751–757. <https://doi.org/10.1016/j.solener.2003.12.009>.

Gupta, P.K., Misal, A., Agrawal, S., 2021. Development of low cost reflective panel solar cooker, *Materials Today: Proceedings, Mater. Today: Proc.* <https://doi.org/10.1016/j.matpr.2020.12.004>

Harmim, A., Merzouk, M., Boukar, M., Amar, M., 2012. Performance study of a box-type solar cooker employing an asymmetric compound parabolic concentrator. *Energy* 47 (1), 471–480. <https://doi.org/10.1016/j.energy.2012.09.037>.

Hosseinzadeh, M., Faezian, A., Mirzababae, S.M., Zamani, H., 2020. Parametric analysis and optimization of a portable evacuated tube solar cooker. *Energy* 194, 116816. <https://doi.org/10.1016/j.energy.2019.116816>.

Hussein, H.M.S., El-Ghetany, H.H., Nada, S.A., 2008. Experimental investigation of novel indirect solar cooker. *Energy Convers. Manage.* 49, 2237–2246. <https://doi.org/10.1016/j.enconman.2008.05.010>.

- 1016/j.enconman.2008.01.026.
- Jaramillo, O.A., Huelsz, G., Hernandez-Luna, G., del Rio, J.A., Acosta, R., Arriaga, L.G., 2007. Solar oven for intertropical zones: optogeometrical design. *Energy Convers. Manage.* 48 (10), 2649–2656. <https://doi.org/10.1016/j.enconman.2007.04.021>.
- Khallaf, A.M., Tawfik, M.A., El-Sebaei, A.A., Sagade, A.A., 2020. Mathematical modeling and experimental validation of the thermal performance of a novel design solar cooker. *Sol. Energy* 207, 40–50. <https://doi.org/10.1016/j.solener.2020.06.069>.
- Kim, Y.S., Balkoski, K., Jiang, L., Winston, R., 2013. Efficient stationary solar thermal collector systems operating at a medium-temperature range. *Appl. Energy* 111, 1071–1079. <https://doi.org/10.1016/j.apenergy.2013.06.051>.
- Kurt, H., Deniz, E., Recebli, Z., 2008. An Investigation into the effects of box geometries on the thermal performance of solar cookers. *Int. J. Green Energy* 5 (6), 508–519. <https://doi.org/10.1080/15435070802498473>.
- Lahkar, P.J., Bhamu, R.K., Samdarshi, S.K., 2012. Enabling inter-cooker thermal performance comparison based on cooker opto-thermal ratio (COR). *Appl. Energy* 99, 491–495. <https://doi.org/10.1016/j.apenergy.2012.05.034>.
- Lahkar, P.J., Samdarshi, S.K., 2010. A review of the thermal performance parameters of box type solar cookers and identification of their correlations. *Renew. Sustain. Energy Rev.* 14 (6), 1615–1621. <https://doi.org/10.1016/j.rser.2010.02.009>.
- Grupp, M., Montagne, P., Wackernagel, M., 1991. A novel advanced box-type solar cooker. *Sol. Energy* 47 (2), 107–113.
- Mawire, A., Lentswe, K., Owusu, P., Shobo, A., Darkwa, J., Calautit, J., Worall, M., 2020. Performance comparison of two solar cooking storage pots combined with wonderbag slow cookers for off-sunshine cooking. *Sol. Energy* 208, 1166–1180. <https://doi.org/10.1016/j.solener.2020.08.053>.
- Mirdha, U.S., Dhariwal, S.R., 2008. Design optimization of solar cooker. *Renew. Energy* 33 (3), 530–544. <https://doi.org/10.1016/j.renene.2007.04.009>.
- Mullick, S.C., Kandpal, T.C., Saxena, A.K., 1987. Thermal test procedure for box-type solar cookers. *Sol. Energy* 39 (4), 353–360. [https://doi.org/10.1016/S0038-092X\(87\)80021-X](https://doi.org/10.1016/S0038-092X(87)80021-X).
- Nandwani, S.S., Fernandez Gomez, O., 1993. Comparative study of conventional and SBICI cardboard solar ovens. *Renew. Energy* 3 (6–7), 607–620.
- Olwi, I.A., Khalifa, A.M.A., 1993. Numerical modeling and experimental testing of a solar grill. *J. Sol. Energy Eng.* 115 (2), 5–10. <https://doi.org/10.1115/1.2930025>.
- Ruivo, C., 2017. On the construction and users acceptance of funnel concrete solar cooker, 6th SCI World Conference, 16–18 January 2017. Vadodara, Gujarat, India.
- Ruivo, C., Carrillo-Andrés, A., Apaolaza-Pagoaga, X., 2021. Experimental determination of the standardised power of a solar funnel cooker for low sun elevations. *Renew. Energy* 170, 364–374. <https://doi.org/10.1016/j.renene.2021.01.146>.
- Sagade, A.A., Samdarshi, S.K., Lahkar, P.J., 2019. Ensuring the completion of solar cooking process under unexpected reduction in solar irradiance. *Sol. Energy* 179, 286–297. <https://doi.org/10.1016/j.solener.2018.12.0.69>.
- Sagade, A.A., Samdarshi, S.K., Lahkar, P.J., Sagade, N.A., 2020. Experimental determination of the thermal performance of a solar box cooker with modified cooking pot. *Renew. Energy* 150, 1001–1009. <https://doi.org/10.1016/j.renene.2019.11.114>.
- Sagade, A.A., Samdarshi, S.K., Panja, P.S., 2018a. Experimental determination of effective concentration ratio for solar box cookers using thermal tests. *Sol. Energy* 159, 984–991. <https://doi.org/10.1016/j.solener.2017.11.021>.
- Sagade, A.A., Samdarshi, S.K., Panja, P.S., 2018b. Enabling rating of intermediate temperature solar cookers using different working fluids as test loads and its validation through a design change. *Sol. Energy* 171, 354–365. <https://doi.org/10.1016/j.solener.2018.06.088>.
- Saxena, A., Agarwal, N., 2018. Performance characteristics of a new hybrid solar cooker with air duct. *Sol. Energy* 159, 628–637. <https://doi.org/10.1016/j.solener.2017.11.043>.
- Saxena, A., Cuce, E., Tiwari, G.N., Kumar, A., 2020. Design and thermal performance investigation of a box cooker with flexible solar collector tubes: An experimental research. *Energy* 206, 118144. <https://doi.org/10.1016/j.energy.2020.118144>.
- SCI, 2020a. Solar Cookers International, Solar Cooking Wiki, Cookit. <https://solarcooking.fandom.com/wiki/Cookit> (accessed February 5, 2021).
- SCI, 2020c. Solar Cookers International, Solar Cooking Wiki, Lightoven III. [https://solarcooking.fandom.com/wiki/Lightoven\\_III](https://solarcooking.fandom.com/wiki/Lightoven_III) (accessed February 5, 2021).
- SCI, 2020d. Solar Cookers International, Solar Cooking Wiki, Teong Tan. [https://solarcooking.fandom.com/wiki/Teong\\_Tan](https://solarcooking.fandom.com/wiki/Teong_Tan) (accessed February 5, 2021).
- SCI, 2021a. Solar Cookers International, Solar Cooking Wiki, Haines 2.0. [https://solarcooking.fandom.com/wiki/Haines\\_2.0](https://solarcooking.fandom.com/wiki/Haines_2.0) (accessed February 5, 2021).
- SCI, 2021b. Solar Cookers International, Solar Cooking Wiki, Hotpot. <https://solarcooking.fandom.com/wiki/HotPot> (accessed February 5, 2021).
- Sethi, V.P., Pal, D.S., Sumathy, K., 2014. Performance evaluation and solar radiation capture of optimally inclined box type solar cooker with parallelepiped cooking vessel design. *Energy Convers. Manage.* 81, 231–241. <https://doi.org/10.1016/j.enconman.2014.02.041>.
- Singh, O., 2021. Development of a solar cooking system suitable for indoor cooking and its exergy and enviroeconomic analyses. *Sol. Energy* 217, 223–234. <https://doi.org/10.1016/j.solener.2021.02.007>.
- Singh, H., Gagandeep, Saini, K., Yadav, A., 2015. Experimental comparison of different heat transfer fluid for thermal performance of a solar cooker based on evacuated tube collector. *Environ. Dev. Sustain.* 17 (3), 497–511. <https://doi.org/10.1007/s10668-014-9556-3>.
- Singh, M., Sethi, P., V., 2018. On the design, modelling and analysis of multi-shelf inclined solar cooker-cum-dryer. *Solar Energy* 162, 620–636. <https://doi.org/https://doi.org/10.1016/j.solener.2018.01.045>.
- Stumpf, P., Balzar, A., Eisenmann, W., Wendt, S., Ackermann, H., Vajen, K., 2001. Comparative measurements and theoretical modelling of single- and double-stage heat pipe coupled solar cooking systems for high temperatures. *Sol. Energy* 71 (1), 1–10. [https://doi.org/10.1016/S0038-092X\(01\)00026-3](https://doi.org/10.1016/S0038-092X(01)00026-3).
- Tawfik M.A., Sagade, A.A., Palma-Behnke, R., Abd-Allah, W.E., El-Shal, H.M., Solar cooker with tracking-type bottom reflector: An experimental thermal performance evaluation of a new design. *Solar Energy* 220, 295–315. <https://doi.org/10.1016/j.solener.2021.03.063>.
- Thamizharasu, P., Shanmugan, S., Gorjian, S., Pruncu, C.I., Essa, F.A., Panchal, H., Harish, M., 2020. Improvement of thermal performance of a solar box type cooker using SiO<sub>2</sub>/TiO<sub>2</sub> nanolayer. *Silicon*. <https://doi.org/10.1007/s12633-020-00835-1>.
- Tiwari, G.N., Yadav, Y.P., 1986. A new solar cooker design. *Energy Convers. Manage.* 26 (1), 41–42.
- UN, 2021. United Nations, Department of Economic and Social Affairs Sustainable Development. <https://sdgs.un.org/goals> (accessed February 5, 2021).
- Zamani, H., Mahian, O., Rashidi, I., Lorenzini, G., Wongwises, S., 2017. Exergy optimization of a double-exposure solar cooker by response surface method. *J. Thermal Sci. Eng. Appl.* 9 (1), 011003. <https://doi.org/10.1115/1.4034340>.
- Zhao, Y., Zheng, H., Sun, B., Li, C., Wu, Y., 2018. Development and performance studies of a novel portable solar cooker using a curved Fresnel lens concentrator. *Sol. Energy* 174, 263–272. <https://doi.org/10.1016/j.solener.2018.09.007>.
- SCI, 2020b. Solar Cookers International, Solar Cooking Wiki, Copenhagen Solar Cooker Light. (Accessed 5 Feb 2021).